http://ansinet.com/itj

ITJ

ISSN 1812-5638

INFORMATION TECHNOLOGY JOURNAL

ANSInet
Asian Network for Scientific Information
308 Lasani Town, Sargodha Road, Faisalabad - Pakistan

Information Technology Journal 10 (6): 1234-1239, 2011
ISSN 1812-5638 / DOI: 10.3923/itj.2011.1234.1239

Frequency Domain Subspace Decomposition Realization of UWB Synchronization Based on PSO

Yang Zhuo, Guo Li-li and Wan Jian
College of information and Communication Engineering,
Harbin Engineering University, Harbin, 150001, China

Abstract: In UWB systems, the power of the signals are attenuated and dispersed when received due to the multi path experience, which makes it difficult to achieve synchronization. In order to make the UWB signal received efficiently and reliably, we proposed a fine symbol synchronization algorithm. Making use of the feature of UWB signal in frequency domain subspace, the algorithm takes advantage of Particle Swarm Optimization to achieve signal synchronization. In the algorithm the synchronous deviation is estimated with the help of frequency domain subspace decomposition and is optimized by Particle Swarm Optimization. The algorithm is of low complexity and can easily be applied to engineering. The simulation results show that the proposed algorithm has a better performance compared to the synchronization algorithm based on singular value decomposition. With low complexity and high performance, the proposed synchronization algorithm can make the UWB signal received efficiently and reliably.

Key words: Ultra-wide band, fine symbol synchronization, frequency domain SVD, particle Swarm optimization

INTRODUCTION

There has been great interest in ultra-wide band (UWB) technology in recent years (Win and Scholtz, 1998; Tingting *et al*., 2009), for its low transmit power, high transmission rate and high system capacity. In Impulse Radio UWB (IR-UWB) systems, a sequence of very short duration pulses, which are called monocycles, are used in communication to gain extremely large transmission bandwidths (Nie and Chen, 2008). As a result synchronization is an important problem to be solved. However, in realistic situation, the power of UWB signals with low power spectral density are attenuated and dispersed when received, due to the multipath experience, which makes it difficult to achieve synchronization. As a result implementation of fast and reliable synchronization is the key to normal communication, as well as a challenge for UWB application.

There has been lots of research on algorithms of synchronization in UWB systems. Synchronization algorithms based on non-coherent receiver can gain high performance. However, the template signal in the receiver is hard to design, for both the linear and the nonlinear distortion of the signal when transmitted (He and Tepedelenlioglu, 2006). Cardoso (2003) proposed a synchronization algorithm based on the dirty template. The algorithm is of low complexity at the expense of the synchronization performance. In Maravic and Vetterli (2003), frequency domain subspace decomposition was used in non-coherent signal synchronization. The algorithm can achieve synchronization with high speed and low complexity. However, the algorithm could not get good performance because it did not make full use of the statistical information of the received signal.

In this study, a fine symbol synchronization algorithm with training bits is proposed. Based on the feature of UWB signal in frequency domain subspace, the algorithm takes advantage of Particle Swarm Optimization to achieve signal synchronization.

SYSTEM MODELING

In IR-UWB system, monocycles, which are of nanosecond scale, are used to transmit information in extremely large transmission bandwidths. Research was carried out based on the UWB system with DS-PAM modulation (Benedetto and Giancola, 2004).

Considering the single user case, the monocycle represented as g (t) is a pulse with the length of D_g in the time domain. Every transmitted symbol waveform without modulation can be described by:

Corresponding Author: Yang Zhuo, College of information and Communication Engineering, Harbin Engineering University, Harbin, 150001, China

$$p_S(t) = \sum_{i=0}^{N_f-1} c_i g(t - iT_f) \quad (1)$$

Every information symbol is conveyed by N_f repeated pulses, with one pulse per frame of duration T_f. $c_0, c_1, \ldots, c_{Nf-1}$ represents the user's pseudo-random direct-sequence (DS) code to enable multiple access and $c_i \in \{-1, 1\}$. The transmitted binary PAM UWB signal can be expressed as:

$$s(t) = \sum_j b_j \cdot p_S(t - jT_s) \quad (2)$$

where, T_s is the symbol duration and $T_s = N_f T_f$. $b_j \in \{-1, 1\}$ is the binary information data of the j-th symbol with equal probability.

Based on Saleh-Valenzuela (S-V) model, IEEE 802.15.4a group for sensor networks proposed the channel model. The Channel Impulse Response (CIR) can be expressed as follows:

$$h(t) = \sum_{l=0}^{L-1} \alpha_l \delta(t - \sigma_l) \quad (3)$$

where, L is the number of paths. $\delta(t)$ is the impulse function. α_l and τ_l are the gain and the delay of the l-th path. And $\sigma_0 = 0$, without considering the case of transmission delay.

Considering the multi-user case, transmitted through the multi-path channel, the received signal can be expressed as:

$$y(t) = \sum_j b_j p_R(t - jT_s) + w(t) + m(t) \quad (4)$$

where, $p_R(t) = p_S(t) \otimes h(t)$ is the waveform which $p_S(t)$ turns into after the channel. "$\otimes$" denotes signal onvolution. w (t) is the multi-user interference. m (t) is the thermal noise.

In the case that the number of the users in the communication is large enough and the power of each user is in the same scale, according to the central limit theory, the multi-user interference is Gaussian random process with zero mean (Win and Scholtz, 1998, 2000). As a result, Eq. 4 can be written as:

$$y(t) = \sum_j b_j p_R(t - jT_s) + u(t) \quad (5)$$

where, $u(t) = w(t) + m(t)$ is Additive White Gaussian Noise (AWGN) with zero mean and a two-side spectrum density of $N_0/2$.

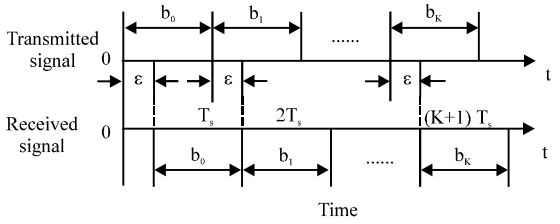

Fig. 1: The schematic diagram of synchronous deviation

Transmission delay exists when the signal is transmitted. After coarse synchronization, there is also synchronous deviation ε, whose value takes real numbers in range $0 \le \varepsilon < T_s$ as shown in Fig. 1. The role of the proposed synchronization algorithm is to obtain the synchronization parameter ε.

SYNCHRONIZATION ALGORITHM

Here, a synchronization algorithm based on frequency domain subspace decomposition (FD-subspace) is proposed firstly. Then, on the basis of FD-subspace, we proposed an optimized synchronization algorithm with the help of Particle Swarm Optimization (PSO-FD-subspace).

Frequency domain subspace decomposition realization of UWB synchronization: According to Fig. 1, when training bits is sent whose value is 1 and length is K+1, the received waveform of the i-th bit can be expressed as $r_i(t)$, where $(I-1)T_s \le t < iT_s$. Sampled with frequency f_c, $r_i(t)$ turns into $r_i[n]$, which can be described by:

$$r_i[n] = p_S[(n-\eta)_N] \otimes h[n] + u[n] = p_S[(n-\eta)_N] \otimes \sum_{l=0}^{L} \alpha_l \delta[n - \tau_l] + u[n] \quad (6)$$

where, $p_S[n]$, h [n] and u [n] are the waveforms $p_S(t)$ h (t) and u (t) turns into after sampled with frequency f_c, with N sampling points. $N = [t \times f_n]$, $\eta = [\varepsilon \times f_n]$, $\tau_l = [\sigma_l \times f_n]$, where [x] is the downward rounding of x. $p_S[(n-\eta)_N]$ is the cyclic shift of $p_S[n]$.

After N point DFT transform Eq. 6 changes into:

$$R_i[k] = P_S[k] \cdot W_N^{k\eta} \cdot \sum_{l=0}^{L} \alpha_l W_N^{k\tau_l} + U[k] = P_S[k] \cdot \sum_{l=0}^{L} \alpha_l W_N^{k(\tau_l+\eta)} + U[k] \quad (7)$$

where, $R_i[k]$, $P_S[k]$ and U [k] are signals $r_i[n]$, $p_s[n]$ and u [n] turns into after point DFT transform. W_N can be expressed as:

$$W_N = e^{-j\frac{2\pi}{N}}$$

$H_i[k]$ is defined as:

$$H_i[k] = R_i[k] / P_S[k] = \sum_{l=0}^{L} \alpha_l W_N^{k(\tau_l+\eta)} + U[k] / P_S[k] \quad (8)$$

Taking advantage of the information in the i-th bit of the training bits, define a P×Q matrix J_i as:

$$J_i = \begin{bmatrix} H_i[1] & H_i[2] & \cdots & H_i[Q] \\ H_i[2] & H_i[3] & \cdots & H_i[Q+1] \\ \vdots & \vdots & \ddots & \vdots \\ H_i[P] & H_i[P+1] & \cdots & H_i[P+Q-1] \end{bmatrix} \quad (9)$$

where, P+Q-1 ≤N and P, Q≥L. J_i can be written as follows:

$$J_i = U_i \Lambda_i V_i^H \quad (10)$$

where, $(\bullet)^H$ denotes conjugate compose. Considering the noise-free case only, define w_l as $Wl = W^{\tau l+\eta}{}_N$, and Ui, Λ_i and V_i can be described as:

$$U_i = \begin{bmatrix} 1 & 1 & \cdots & 1 \\ w_0 & w_1 & \cdots & w_{L-1} \\ \vdots & \vdots & \ddots & \vdots \\ w_0^{P-1} & w_1^{P-1} & \cdots & w_{L-1}^{P-1} \end{bmatrix}$$

$$\Lambda_i = \mathrm{diag}(\alpha_0, \alpha_1, \cdots, \alpha_{L-1})$$

$$V_i = \begin{bmatrix} w_0 & w_1 & \cdots & w_{L-1} \\ w_0^2 & w_1^2 & \cdots & w_{L-1}^2 \\ \vdots & \vdots & \ddots & \vdots \\ w_0^Q & w_1^Q & \cdots & w_{L-1}^Q \end{bmatrix}$$

Seen from the analyses above, U_i, Λ_i and V_i have the rank L, so does J_i. And U_i, V_i are both Vandermonde matrices. Matrix Φ is defined as Φ = diag (w_0, w_1,..., w_{L-1}). According to properties of Vandermonde matrix, the following formulas can be established:

$$\begin{cases} U_i^+ = U_i^- \cdot \Phi \\ V_i^+ = V_i^- \cdot \Phi \end{cases} \quad (11)$$

where, $(\bullet)^+$ and $(\bullet)^-$ donate the operations of omitting the first and last row of matrix (•).

According to Eq. 11, U_i and V_i satisfy the shift-invariant subspace property. Further more, the submatrices which U_i and V_i turns into after omitted the first rows or last rows have full column rank and satisfy the shift-invariant subspace property if P-m ≥L, Q-m≥L. Define (•) and $\underline{(\bullet)}$ as operations of omitting the first rows or last rows of matrix (•). The synchronous deviation can be obtained by calculating the phase angle of the smallest eigenvalue of matrix $\underline{U_i}^{\dagger}\overline{U_i}$. In the noise-free case, making use of the i-th bit of the training bits, $\hat{\eta}_{Si}$ which is the estimate value of the synchronous deviation η, can be described as:

$$\hat{\eta}_{Si} = \frac{2\pi}{N} \cdot \angle \min\left(\mathrm{eig}\left(\underline{U_i}^{\dagger}\overline{U_i}\right)\right) \quad (12)$$

where $(\bullet)^{\dagger}$ is the pseudo inverse matrix of (•). eig (•) is the eigenvalue of matrix (•). ∠ donate the operation of calculating the phase angle.

Taking noise into consideration, after the singular value decomposition, J_i can be expressed as:

$$J_i = U_{Ri} \Lambda_{Ri} V_{Ri}^H \quad (13)$$

where, U_{Rj} and V_{Rj} are the left and right singular matrix of J_i. Λ_{Ri} is a P×Q matrix, which can be expressed as:

$$\Lambda_{Ri} = \begin{bmatrix} \Lambda_{Si} & 0_{L\times(Q-L)} \\ 0_{(P-L)\times L} & 0_{(P-L)\times(Q-L)} \end{bmatrix}$$

where, Λ_{Si} is a L×L diagonal matrix which is composed of L singular values. U_{Si} is defined as the first L columns of U_{Ri}. Then the signal subspace of matrix J_i can be estimated by U_{Si}. According to the analyses above, U_i in Eq. 10 can be replaced by U_{Si}, when synchronization is performed. In the case that noise exists, taking advantage of the i-th bit of the training bits, $\hat{\eta}_i$ which is the estimate value of the synchronous deviation η, can be described as:

$$\hat{\eta}_i = \frac{2\pi}{N} \cdot \angle \min(\mathrm{eig}(\underline{U_{Si}}^{\dagger}\overline{U_{Si}})) \quad (14)$$

Making use of the expectation of $\hat{\eta}_i$, $\hat{\eta}$ which is the final estimated value of the synchronous deviation can be expressed as:

$$\hat{\eta} = \frac{1}{K+1} \sum_{i=0}^{K} \hat{\eta}_i \quad (15)$$

where, K+1 is the length of the training bits.

Optimized frequency domain subspace decomposition UWB synchronization based on PSO: Particle Swarm Optimization (PSO) is used for solving the optimization problem originally inspired by certain social behavior of bird flocking (Kennedy and Eberhart, 1995). In PSO individuals which are called as particles, fly through the solution space with a certain trajectory. Under the guidance of its own and its neighbors' experience, each particle will gradually fly into the area of global optimum.

In n-dimensional space, $X_i = (x_{i1}, x_{i2},..., x_{in})$ is the position vector of the i-th particle and $V_i = (v_{i1}, v_{i2},..., v_{in})$ is the velocity vector of the i-th particle. $P_i = (p_{i1}, p_{i2},..., p_{in})$ and $P_g = (p_{g1}, p_{g2},..., p_{gn})$ represented the individual best

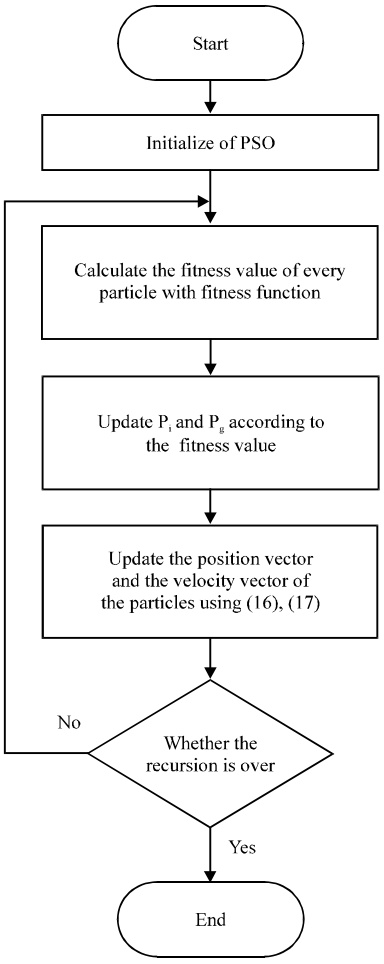

Fig. 2: The flow chart of PSO

position of the i-th particle and the global best position discovered by the whole swarm. Using the fitness function fitness = f (X_i), P_i and P_g can be calculated. PSO can be described as the following update equations:

$$v_{ij}^{(t+1)} = v_{ij}^{(t)} + c_1 r_1 (p_{ij}^{(t)} - x_{ij}^{(t)}) + c_2 r_2 (p_{gj}^{(t)} - x_{ij}^{(t)}) \quad (16)$$

$$x_{ij}^{(t+1)} = x_{ij}^{(t)} + v_{ij}^{(t+1)} \quad (17)$$

where, i and j is used to represent the indexes of the i th particle in the j th dimension. t stands for iteration times. c_1 and c_2 are constant values that are called personal and global accelerations. r_1 and r_2 are uniform random numbers in the range [0, 1]. In 2007, Bratton and Kennedy (2007) proposed a better method of parameter settings of PSO, which is called Standard Particle Swarm Optimization (SPSO). In this study, parameters are set as SPSO. The flow chart of PSO is shown in Fig. 2.

According to the analysis above, an optimized synchronization algorithm with the help of Particle Swarm Optimization (PSO-FD-subspace) is proposed. PSO can be used to optimize the estimated value $\hat{\eta}_i$ obtained from the training bits. The fitness function is set on the basis of the least mean square criterion, $\hat{\eta}_{PSO}$ which is the final estimated value of the synchronous deviation, can be obtained by the following equation:

$$\hat{\eta}_{PSO} = \underset{\hat{\eta}_e}{\operatorname{argmin}} \left[\frac{1}{K+1} \sum_{i=0}^{k} (\hat{\eta}_e - \hat{\eta}_i)^2 \right] \quad (18)$$

where, $\hat{\eta}_e$ is the intermediate variable in the iteration. And the fitness function can be written as:

$$f(\hat{\eta}_e) = \frac{1}{K+1} \sum_{i=0}^{k} (\hat{\eta}_e - \hat{\eta}_i)^2 \quad (19)$$

As a result, the optimization problem of synchronization can be transformed into solving the minimum fitness value in PSO.

SIMULATION RESULTS

Simulations are carried out based on CM1 by the IEEE802.15.3a channel modeling subcommittee (Foerster, 2003). The system parameters are set as T_s = 200 nsec, T_f = 40 nsec, N_f = 5. The second derivative of a Gaussian function is chosen as the monocycle pulse with its duration T_m = 0.6 nsec. The performance of the proposed algorithm can be shown through two experiments.

The first experiment shows the performance of FD-subspace for different length of training bits. In the figure NMSE is used as ordinate and noise ratio (SNR) which can be expressed by Eb/N0 is used as abscissa. Compared with the SVD synchronization algorithm proposed by Maravic and Vetterli (2003, FD-subspace is better in synchronization. From Fig. 3 the performance of FD-subspace is improved, as the length of the training bits increases. However, the performance improves slowly, when the number of the training bits is more than 60. As a result, 60 is the optimum number of the training bits in FD-subspace.

The second experiment shows the performance of PSO-FD-subspace for different length of training bits which is showed in Fig. 4. The figure shows PSO-FD-subspace is better than SVD synchronization algorithm in synchronization. From Fig. 4 the performance of PSO-FD-subspace is improved, as the length of the training bits increases. And 60 is also the optimum number of the training bits in PSO-FD-subspace, as the performance

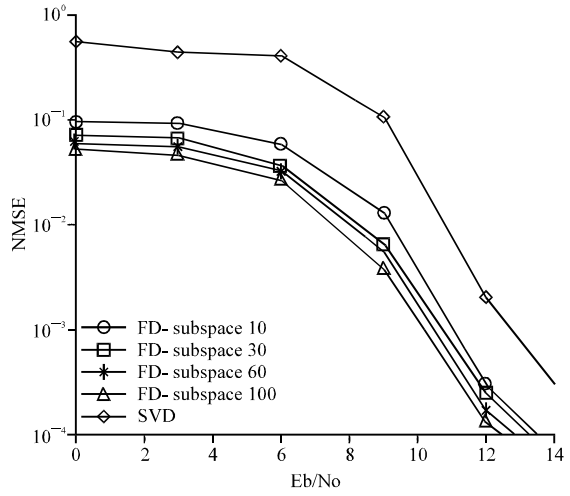

Fig. 3: The performance of FD-subspace for different length of training bits

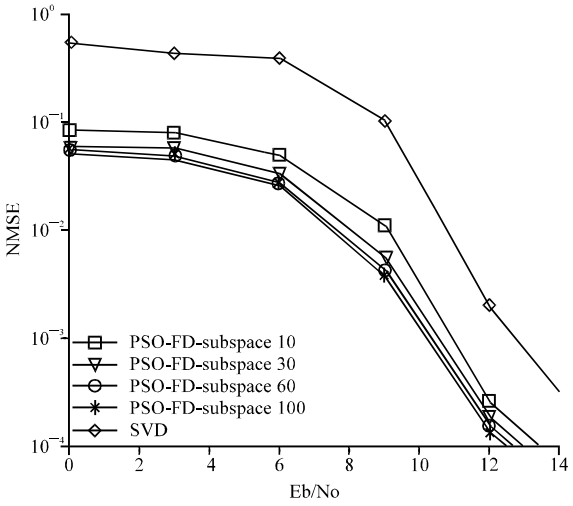

Fig. 4: The performance of PSO-FD-subspace for different length of training bits

improves slowly, when the number of the training bits is more than 60. Similar trend in the performance curves of FD-subspace and PSO-FD-subspace can be found in Fig. 3 and Fig. 4. The representative differences of the two synchronization algorithms in detail are showed in Fig. 5. When the length of the training bits is same, the NMSE performance of PSO-FD-subspace is better than that of FD-subspace. The comparison shows PSO-FD-subspace can perform synchronization with fewer training bits. As a result, PSO-FD-subspace has better performance compared with FD-subspace.

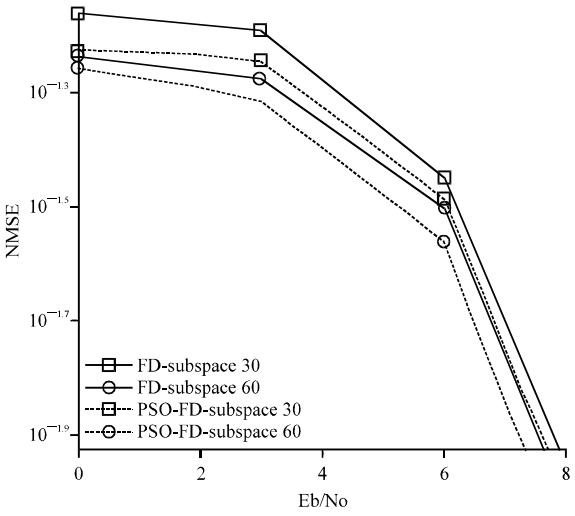

Fig. 5: NMSE with E_b/N_0 in different synchronization algorithms

CONCLUSIONS

In this study, a fine symbol synchronization algorithm based on frequency domain subspace decomposition (FD-subspace) is introduced. With the help of PSO, an optimized synchronization algorithm on the basis of FD-subspace is proposed. Both of them are good in performance of synchronization with low complexity. Compared with FD-subspace, PSO-FD-subspace can perform synchronization with fewer training bits.

ACKNOWLEDGMENTS

This study is sponsored by National Natural Science Foundation of China with grant number 60772129 and Special Foundation Project of Harbin technological innovation under grant 2010RFQXG030.

REFERENCES

Benedetto, M.G.D. and G. Giancola, 2004. Understanding Ultra Wide Band Radio Fundamentals. Prentice Hall, USA.

Bratton, D. and J. Kennedy, 2007. Defining a standard for particle swarm optimization. Proceeding of the Swarm Intelligence Symposium, April 1-5, Honolulu, HI, pp: 120-127.

Cardoso, J.F., 2003. Correlation and gaussianity in independent component analysis. J. Mach. Learn. Res., 4: 1177-1203.

Foerster, J., 2003. Channel modeling sub-committee report. IEEE P802.15 Wireless Personal Area Networks, P802.15-02/490r1-SG3a.

He, N. and C. Tepedelenlioglu, 2006. Performance analysis of Non-coherent UWB recevers at different synchronization levels. IEEE Trans. Wirel. Commun., 5: 1266-1273.

Kennedy, J. and R. Eberhart, 1995. Particle swarm optimization. Proceedings of the IEEE International Conference on Neural Networks, Nov. 27-Dec. 1, Piscataway, New Jersey, pp: 1942-1948.

Maravic, I. and M. Vetterli, 2003. Low-complexity subspace methods for channel estimation and synchronization in ultra-wideband systems. Proceedings of the International Workshop on Ultra-Wideband Systems, (IWUWB'03), Berkeley, CA, pp: 1-5.

Nie, H. and Z. Chen, 2008. Transceiver technologies for impulse radio ultra wideband (IR-UWB) wireless systems. Proceeding of the Communication Networks and Services Research Conference (CNSR), May 5-8, Halifax, NS, pp: 3-4.

Tingting, Z., Z. Qinyu, Z. Naitong and X. Hongguang, 2009. Performance analysis of an indoor UWB ranging system. J. Syst. Eng. Electron., 20: 450-456.

Win, M.Z. and R.A. Scholtz, 1998. Impulse radio: How it works. IEEE Commun. Lett., 2: 36-38.

Win, M.Z. and R.A. Scholtz, 2000. Ultra-wide band width timehopping spread spectrum impulse radio for wireless multiple-access communications. IEEE Trans. Commun., 48: 679-691.